DESIGN AND VERIFICATION OF THE ATTITUDE DETERMINATION AND CONTROL ALGORITHMS FOR THE SOURCE CUBESAT

P. J. Haufe*, J. Goll*, C. Luckas*, L. Lauer*, N. Bürger*, L. Wolfgramm*, N. Pentke*, F. Tuttas†, D. Galla ‡, M. Kanzow‡, M. Eggert‡, S. Klinkner‡

* KSat e.V., University of Stuttgart, Germany
† Institute of Flight Mechanics and Controls, University of Stuttgart, Germany
‡ Institute of Space Systems, University of Stuttgart, Germany

Abstract

The Stuttgart Operated University Research Cubesat for Evaluation and Education is a 3U+ CubeSat that is entirely built by students of the Small Satellite Student Society and supervised by the Institute of Space Systems, both at the University of Stuttgart. In addition to education, technology demonstration and meteor observation, its scientific goal is to improve the understanding of small satellite behaviour and the demise process during re-entry. Like many other missions, both academic and non-academic, SOURCE requires a space- and cost-efficient attitude determination and control system. Due to the added educational aspect of a student developed satellite, it is attractive to design most of the systems in-house. The main tasks are detumbling after deployment, sun- and Earth pointing of the solar panels and the meteor camera, and provision of the current attitude for the scientific payloads. The used algorithms are predominantly self-developed or customized to fit the system's needs. Since the actuation is entirely based on magnetorquers, the system is limited to two-axes control. This imposes a unique set of challenges in attitude control and requires rigorous testing in simulations to ensure satisfactory performance of the system, even if individual sensors fail. A solution for early testing of the MATLAB to C++ transpiled code is presented. The development and testing approach for the ADCS software can act as a source of inspiration for future CubeSat projects.

Keywords

CubeSat; ADCS; Magnetorquer-only

Acronyms

ADC	Analogue to Digital Converter
ADCS	Attitude Determination and Control System
COTS	Commercial Off-The-Shelf
DLR	German Aerospace Center
ESA	European Space Agency
FDIR	Failure Detection, Isolation, and Recovery
FIPEX	Flux Phi Probe Experiment
FlatSat	Flat Satellite Test Bench
GAFE	Generic AOCS GNC Techniques and Design Framework for FDIR
GNSS	Global Navigation Satellite System
GYR	Gyroscope
HKB	Housekeeping Board
IRAS	Integrated Research Platform for Affordable Satellites
IRS	Institute of Space Systems
ISS	International Space Station
LEO	Low Earth Orbit
MEKF	Multiplicative Extended Kalman Filter
MEMS	Micro-Electro-Mechanical Systems
MeSHCam	Meteor, Star and Horizon Tracking Camera
MGM	Magnetometer
MTQ	Magnetorquer
OBC	Onboard Computer
QUEST	Quaternion Estimator
SOURCE	Stuttgart Operated University Research CubeSat for Evaluation and Education
SUS	Sun Sensor
TC	Telecommand

1. INTRODUCTION

In the realm of spacecraft technology, the Attitude Determination and Control System (ADCS) plays a pivotal role. By means of sensors and actuators, a spacecraft can precisely measure and adjust its rotational rate and attitude. These functions are imperative for optimizing the use of solar arrays and onboard payloads, such as observational instruments [1]. ADCS algorithms that are tailored to mission-specific requirements process sensor data and calculate control inputs for actuators. Rigorous

doi: 10.25967/610141

testing of these algorithms is paramount to ensure mission success.

With the growing demand for cost-effective Low Earth Orbit (LEO) payload deployment, CubeSats have seen a remarkable surge in development and launch activities [2]. While CubeSats conventionally handle attitude determination, rotational stabilization, and basic sun-pointing tasks, more advanced capabilities such as pointing and handling early phase re-entry conditions are relatively uncommon, particularly in satellites that lack reaction wheels and high-fidelity sensor systems.

The Stuttgart Operated University Research CubeSat for Evaluation and Education (SOURCE) mission sets out to fulfill these tasks while leveraging in-house resources and affordable Commercial Off-The-Shelf (COTS) components. Notably, it is distinguished by its dual objectives: advancing education through a fully student-built satellite and pursuing unique mission goals in meteor observation and re-entry science. As a result, the majority of software and hardware components are developed and rigorously tested in-house to ensure the successful achievement of these ambitious aims.

This paper focuses on the efforts to verify the developed software using time domain simulations conducted in MATLAB/Simulink. More information about the hardware of SOURCE's ADCS can be taken from previously published work [3]. The methods outlined in this paper, both in development and verification, aim to serve as a valuable reference for similar CubeSat missions bound for LEO.

1.1. The CubeSat SOURCE

SOURCE is a joint project of the Institute of Space Systems (IRS) and the Small Satellite Student Society (KSat e.V.), both at the University of Stuttgart. In addition to investigating satellite demise, the project aims to provide a platform for education, technology demonstration and meteor observation [4]. It is supported by the European Space Agency (ESA) Fly Your Satellite! 3 programme. The satellite is a 3U+ CubeSat with dimensions of $10 \times 10 \times 36$ cm and a mass of approximately 4.5 kg. A rendering is shown in FIG 1 and FIG 2 provides an overview of SOURCE's mission.

The payloads are split into 3 categories: cameras, atmospheric and re-entry sensors, and technology demonstrators. The first phase will focus on meteor observations and experimental star tracking using the Meteor, Star and Horizon Tracking Camera (MeSHCam). Starting at 200 km, the early re-entry phase begins and measurements of temperature, heat flux, pressure and atmospheric oxygen will be collected and downlinked. Five sets of pressure, heat, and temperature sensors and two Flux Phi Probe Experiment (FIPEX) atomic oxygen sensors from the University of Stuttgart's High Enthalpy Flow Diagnostics Group will be mounted at various locations on the outside of SOURCE. They are used to study atmospheric composition and satellite disintegration during re-entry.

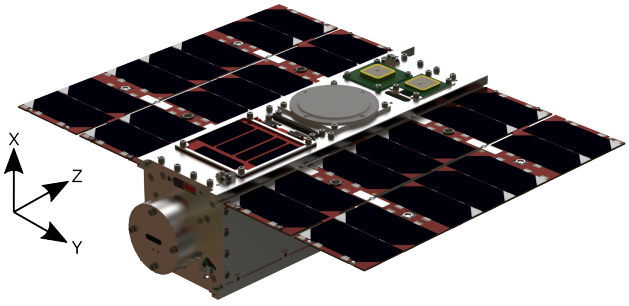

FIG 1. Rendering of SOURCE.

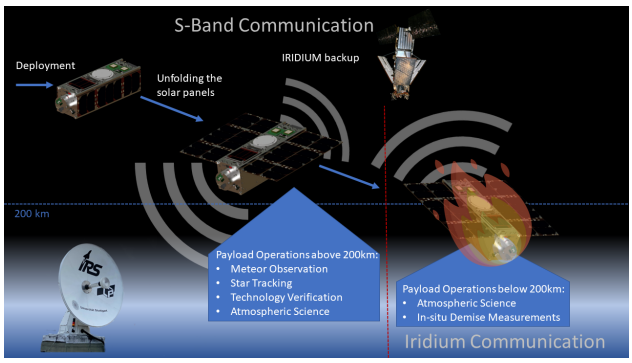

FIG 2. Mission Scenario of SOURCE.

The technology demonstrators include a smart heater from Airbus, a thin film solar cell experiment from the German Aerospace Center (DLR) in Bremen and a multi-purpose CFRP sandwich structure with integrated electronics of the Integrated Research Platform for Affordable Satellites (IRAS) project of the DLR and the Fraunhofer Institute, both in Stuttgart, together with the IRS [5].

To generate power, 56 solar cells produce a maximum of 32 W, which is stored in a *Gomspace BPX* lithium-ion battery. The distribution and regulation is managed by an in-house controller board, centered around the radiation tolerant *Vorago 10820*. SOURCE's on-board computer is an *IOBC* from *ISISpace* with an in-house developed payload computer for camera operation. Primary communications are via an S-band *Syrlinks* transceiver, with an Iridium communication system as a back-up and for ground independent downlinks, during early re-entry data acquisition.

The ADCS is essential not only for pointing the solar arrays and ensuring the general functioning of the system, but also for coarse Earth pointing of the MeSHCam. In addition, the estimated attitude provides an important context for the spatially distributed re-entry and atmospheric measurement sensors.

Attitude control is achieved using three in-house developed, manufactured and tested Magnetorquers (MTQs) as actuators. The COTS Sun Sensors (SUSs), Gyroscopes (GYRs), Magnetometers (MGMs) and the MeSHCam payload camera used as an experimental star tracker are used for attitude determination. Two Global Navigation Satellite System (GNSS) receivers enable orbit determination.

2. ADCS ARCHITECTURE

The following section will serve as an overview of the basic system architecture of the ADCS of SOURCE. Each component will be briefly described. An overview of the system's component placement is given in FIG 3. All sensors are planned to fly soon or have already flown on other missions [3, 6]. The actuators are developed in-house.

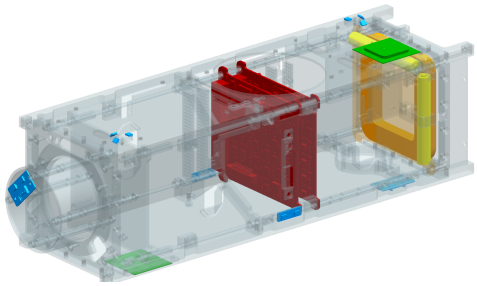

FIG 3. ADCS components on SOURCE: SUS (blue), GNSS antennas (green), housekeeping boards including MGMs, GYRs, sensor interfaces and MTQ control (red), MTQs (orange and yellow).

2.1. Sensors

MGM: SOURCE uses three *RM3100* magnetometers with a sampling frequency of 10 Hz, to measure the local direction and intensity of earths magnetic field.
GYR: Two Micro-Electro-Mechanical Systems (MEMS) gyroscopes in the shape of three axes *BMI270* sensor units measure the rotational rate of SOURCE.
GNSS: A hot-redundant GNSS of two *Skytraq Orion B16*, each connected to a single *Taoglas AP.25E.07.0054A* active patch antenna, provides the ADCS with real time position measurements.
SUS: A total of 16 *OSRAM SFH-2430-Z* photodiodes are used as sun sensors to determine the light intensity in their normal direction. Each diode is protected from UV-degradation by a *Solarglas 0787* cover layer by Schott AG, glued to the photodiodes with space qualified *DOW CORNING 93-500*. The SUS's readings are routed through four *Texas Instruments OPA4196* amplifier and a *Maxim MAX1229* analog to digital converter, placed on the housekeeping boards.

2.2. Actuators

The entire actuation of SOURCE is accounted for by three in-house developed MTQs. In total, there will be one air-core and two cylindrical MTQs with ferromagnetic cores. Due to mass, size and financial constraints, neither thrusters nor reaction wheels could be fitted. As a result, an architecture based purely on magnetic actuation was chosen. MTQ-only systems are constrained by their operating principle and power consumption, resulting in limited pointing efficiency. A detailed account of the characterization and development process of the MTQs is discussed in Maraqten et al. [7]. Flight hardware has already been built and was characterized to have a magnetic dipole moment higher than 0.5 A m^2 [3].

The GYR, MGM and SUS interfaces, Analogue to Digital Converters (ADCs) and the H-Bridge drivers for MTQ control are placed on two in-house developed, soldered and qualified Housekeeping Boards (HKBs).

2.3. Operation Modes

During the operation of SOURCE, different operational modes will be used by the ADCS to achieve nominal bus functionality, scientific measurements and payload operations. A mode transition can be triggered either by Telecommand (TC), changes in the dynamic system state or malfunctions. The five modes are as follows:
Detumble Mode: Following the deployment from the launcher, the Detumble Mode will decrease the rotational rate of SOURCE to enable the deployment of the solar arrays for charging the satellite's batteries. The satellite will enter the Detumble Mode every time the rotational rate increases above 1 $°s^{-1}$. This mode exclusively uses the rotational data provided by derivation of the magnetic field vector to reduce the necessary electrical energy as much as possible.
Safe Mode: This mode is automatically triggered by the OBC when either sensor failures occur or the satellite's battery charge reaches a critically low level. In Safe Mode the ADCS exclusively uses data from the SUS and MGMs to direct the solar panels towards the sun, ensuring maximum power production with minimum power consumption. During the eclipse phase of the orbit, the SUSs cannot be used and only rate damping will be performed, similar to Detumble Mode.
Idle Mode: The nominal mode of operation for the satellite, in which the solar arrays are pointed towards the Sun using all available attitude sensors and the GNSS receiver. This maximizes the accuracy of the determined attitude and thus helps in minimizing the performance error. Unlike Safe Mode, which only performs alignment tasks during the solar phase of the orbit, Idle Mode is capable of controlling SOURCE's attitude during the eclipse.
Pointing Mode: An additional mode enabling inertial pointing of SOURCE for Earth and meteor observation campaigns. This is achieved by changing the target attitude to allow pointing of the MeSHCam (directed along the X^--axis of SOURCE).
Re-entry Mode: As the satellite's orbit decays over the course of the mission, atmospheric disturbances increase and at some point exceed the MTQs capabilities. At around 240 km the ADCS will enter Re-entry Mode [5]. The satellite will use the full range of sensors for position and attitude determination. Whether the satellite will additionally use the MTQs to dampen its rotation and achieve dynamic stability or fully switch them off, is currently being evaluated [8].
The full logic for the transition between the different control laws is shown in FIG 4. An overview of the components used in each of the different modes can be found in TAB 1.

TAB 1. Components used in each ADCS mode.

Mode	SUS	MGM	GYR	GNSS	MTQ
Detumble		X			X
Safe	X	X			X
Idle	X	X	X	X	X
(Pointing)	X	X	X	X	X
Re-entry	X	X	X	X	TBD

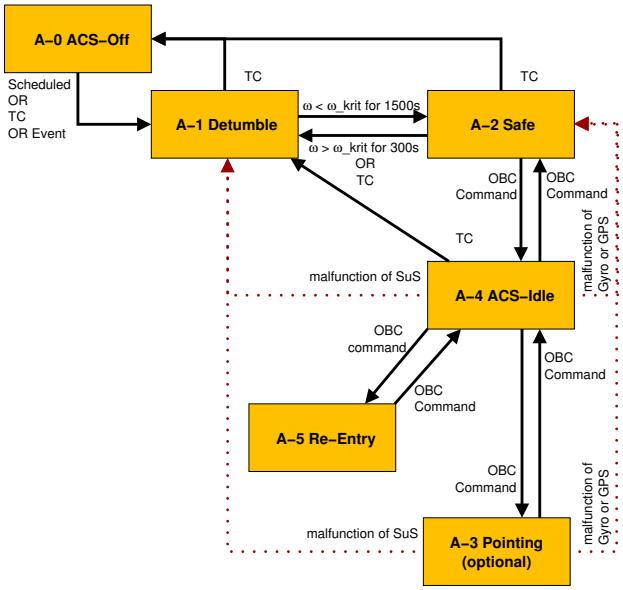

FIG 4. ADCS mode transitions in SOURCE's ADCS.

2.4. System Requirements

Due to the deployable solar array, it is vital that SOURCE's X^+-axis is oriented towards the sun for power generation. The launch provider is yet to be determined and high rotational rates after separation must be anticipated. In Safe and Idle Mode, the primary requirement is to ensure sufficient power generation by pointing the solar panels towards the sun. Secondary objectives are mainly to be achieved in Pointing Mode. They are influenced by the payload: the MeSHCam must be pointed at Earth to make observations at low angular rates, which helps to avoid motion blur. However, the MeSHCam does not need to track specific targets. The FIPEX sensors, which detect atomic oxygen, must be directed towards the incoming flow direction for 120 s during each measurement. In the re-entry science phase, aerodynamic disturbances reach a critical point at an altitude of 240 km, surpassing the static torque capabilities of the MTQ and consequently limiting the attitude control [5]. Nevertheless, pressure, heat flux and FIPEX sensors used for re-entry observations necessitate dependable attitude and orbit determination for contextualizing their data.

The reduced capability of an MTQ-only architecture compared to higher fidelity ADCS systems is also evident in the essential requirements. The following requirements are intended to be verified in the presented work:

REQ-1: Attitude determination accuracy shall be better than 5° in the sun phase of the orbit in Idle Mode.

REQ-2: Rotation rates of up to 90 $°s^{-1}$ per axis after deployment shall be reduced to less than 1 $°s^{-1}$ in less than 5 h in the Detumble Mode.

REQ-3: The normal of the solar arrays shall point towards the sun with an error of less than 20° in the sun phase of the orbit for greater than 68 % of the time in Safe and Idle Mode.

REQ-4: Angular rates shall be kept below 1 $°s^{-1}$ during pointing operations in Safe and Idle Mode.

2.5. Approach

The ADCS key requirements are verified by rigorous testing in simulations using ESA's Generic AOCS GNC Techniques and Design Framework for FDIR (GAFE) [9]. GAFE is employed by SOURCE's ADCS team for its time domain 6-DoF simulation. While its main purpose is to develop and test Failure Detection, Isolation, and Recovery (FDIR) techniques, it also serves as a robust tool for evaluation and verification of an ADCS. GAFE features predefined sensor models, that are enhanced with self-implemented models, to emulate the sensor behavior taken from the manufacturer data sheet and in-house conducted hardware tests. The CubeSat's environment and resulting disturbances are also modelled in GAFE and are customized to the SOURCE mission. Additional models for Earth albedo and aerodynamic drag, based on investigations using Direct Simulation Monte Carlo methods are added [8].

After verification of the core algorithms against the key system requirements in MATLAB, the code is transpiled into C++ and tested using a dedicated C++ simulator. Afterwards, the transition is made to gradually incorporate tests with the real hardware on a satellite test bench. A Flat Satellite Test Bench (FlatSat) is a ground-based testing setup that incorporates the key components and functions of a satellite. It is used to validate and ensure the proper operation of all systems running on flight-like hardware before the flight model is built, tested and launched into space. For SOURCE, the qualification models of the printed circuit boards and sensors will gradually be tested together with the Onboard Computer (OBC) to verify the function of the systems.

3. ATTITUDE DETERMINATION

SOURCE's navigation system is in charge of determining the satellite's position and attitude parameters continuously from commissioning, detumbling, sun- and Earth-pointing phases, up until the re-entry science phase.

3.1. Concept

Using low resolution COTS sensors as described in section 2.1 imposes limitations on the navigation capability of the satellite. The absence of a star tracking device restricts the attainable accuracy of attitude determination to scales of degrees instead of arcseconds. Relying

solely on a constellation comprising two vector measurements poses a challenge during eclipse phases, where no sun vector is present. To sustain reliable attitude determination through these shadow periods, strapdown integration is required. For this purpose, SOURCE uses the quaternion-based Multiplicative Extended Kalman Filter (MEKF) [10]. As illustrated in FIG 5, the filter fuses the angular rate from the gyroscopes with the magnetic field and sun direction measurements as well as their associated mathematical models. These models require an accurate time and position of the satellite, both provided by GNSS receivers.

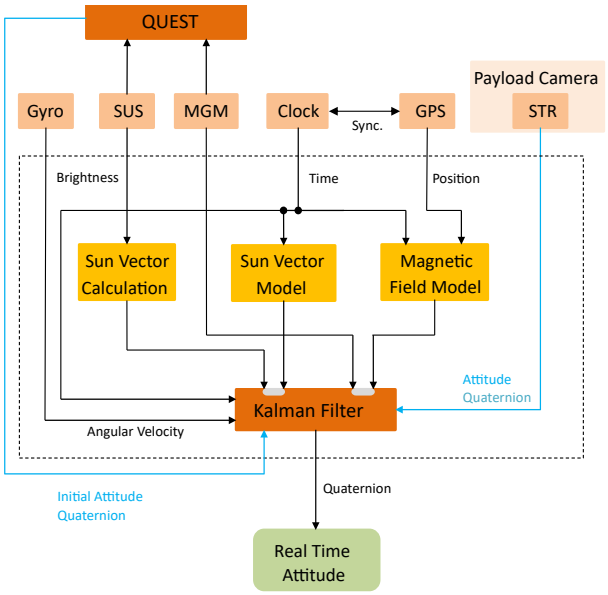

FIG 5. Attitude Determination Concept [11].

Furthermore, the payload's MeSHCam camera serves as an experimental star tracker. The images captured by this camera are subject to processing via a modified version of the open-source tracking software *astrometry.net* [12]. This software has demonstrated successful star tracking capabilities within the arcsecond accuracy range [13], as verified in the DLR's SOFIA project. Since the star tracker will be flight-tested during the SOURCE mission, it is not part of the nominal ADCS. However, it can be integrated into the Kalman Filter during periods when its functionality is not actively engaged in observation campaigns.
The key feature of an Extended Kalman Filter is the ability to estimate non-linear dynamics through linearization. However, initializing the filter with an inaccurate state undermines this assumption, potentially leading to reduced steady-state performance, delayed convergence and potential divergence [14]. To circumvent this issue, the Quaternion Estimator (QUEST) algorithm [10] is utilized to compute the filter's initial state. In addition to the quaternion computation, QUEST also delivers an associated covariance estimation, rendering it more suitable for Kalman Filter initialization in comparison to conventional methods like the Triad algorithm. Simulations have shown that the selected filter is capable of providing sufficient attitude determination accuracy to meet the mission requirements [11].

3.2. Sun Vector Calculation

Determination of the sun vector is vital for sun-pointing in Safe Mode and as an input to the Kalman Filter in Idle Mode. In contrast to traditional sun sensors, the used SUS are not capable of determining a vector with a single diode. Hence, a combination of diodes is necessary to calculate the sun vector. Furthermore, two different arrangements are used, one being the One-Sensor-per-Face (OSPF) and the other being a pyramid-like arrangement of three diodes in an effort to increase the accuracy for sun-facing attitudes. The twelve SUS of the OSPF arrangement are used in most orientations, except when the angle between the sun vector and the X^+-axis is less than 45°. In this case, the pyramid arrangement will be used. This enables a higher accuracy determination during sun pointing of the solar panels. The values of the OSPF sensors are processed and normalized to a sun vector with each pair giving the corresponding X, Y, and Z values. The data of the pyramid SUS is used to calculate the angles between the X^+- and Y^+/Z^+-axes.

$$\psi = \frac{\pi}{4} + \arctan\left(\frac{I_P, Y^-}{I_P, Y^+}\right) \tag{1}$$

$$\theta = \frac{\pi}{4} + \arctan\left(\frac{I_P, Z^-}{I_P, Z^+}\right) \tag{2}$$

In equations 3.2 and 3.2, ψ is the angle between the X^+- and Y^+-axis, θ is the angle between the X^+- and Z^+-axis and I_P is the current produced by the photo diodes in the corresponding direction. SOURCE's axes are depicted in FIG 1. These angles can then be transformed into a sun vector in the body frame of the satellite S, as shown in equation 3.

$$\mathbf{S} = \begin{bmatrix} \sin\psi \cdot \sin\theta \\ \cos\psi \\ \sin\psi \cdot \cos\theta \end{bmatrix} \tag{3}$$

3.2.1. Verification

The verification of the sun vector calculation is carried out with GAFE simulations and testing with a physical model. The achievable accuracy using the GAFE simulation resulted in an overall measurement error of $5\,°$ and a pyramid algorithm error of $3.1\,°$. The results of the tests with the physical model resulted in an overall measurement error of $7.6\,°$ and an error of $4.8\,°$ when the pyramid is used. This discrepancy is caused by real world effects that were not anticipated. A detailed analysis was carried out and can be found in the corresponding paper [15]. The applicable requirement *REQ-1* (estimation error of less than 5°) is met in Safe Mode for the relevant orientation of sun-facing pyramids and solar arrays.

3.3. Multiplicative Extended Kalman Filter

The attitude determination methodology employed for the satellite SOURCE is founded on the MEKF approach as introduced in the work by Markley and Crassidis [10]. A distinguishing feature of this variant of the MEKF resides in its treatment of attitude, parameterised in quaternion form, as a global construct rather than an explicit component within the state vector. Instead, the state vector contains an error characterization of the attitude. Consequently, the overall attitude is updated at each discrete time increment by means of a multiplication operation between the previous attitude estimate and the derived error estimate. This process ensures the maintenance of a unit quaternion.
Conventionally, quaternion representations are widely adopted for describing attitude due to their intrinsic advantages such as circumvention of singularities and minimal dimensionality. Nevertheless, it is important to note, that for exceedingly small rotational deviations, three-dimensional representations also remain viable [10]. Such alternate representations offer the potential for computational alleviation by reducing the dimensionality of matrices. Thus, the attitude error is expressed as a three-dimensional rotation vector $\boldsymbol{\vartheta}$. The resulting global and local state vectors are given by

$$\mathbf{x} = \begin{bmatrix} \mathbf{q} \\ \boldsymbol{\beta} \end{bmatrix} \qquad \Delta\mathbf{x} = \begin{bmatrix} \boldsymbol{\delta\vartheta} \\ \Delta\boldsymbol{\beta} \end{bmatrix} \tag{4}$$

where $\boldsymbol{\beta}$ denotes the gyroscope bias and the quaternion attitude state is denoted by $\mathbf{q}$.
The incorporation of angular rate information is fundamental for predicting the orientation at the subsequent time step. Typically, this data is sourced from a dynamic model, which factors in all the deviation torques of the space environment as well as the internal torques caused by the actuators of the spacecraft. However, the precision with which these deviations can be determined, along with the spacecraft's inertia matrix, inherently carries limitations that could potentially impact the filter's performance [10]. Particularly considering the constrained financial resources and limited testing capacities of a student CubeSat mission, it is decided to utilize a kinematic quaternion propagation technique using the gyroscope measurements. This bears not only the advantage of simplifying implementation but also leads to a reduction in computational demands by negating the requirement for numerical integration.
To effectively mitigate the influence of bias and noise perturbing the angular rate measurements, the filter incorporates a gyroscope model, formulated as follows:

$$\boldsymbol{\omega}(t) = \boldsymbol{\omega}^{true}(t) + \boldsymbol{\beta}^{true}(t) + \boldsymbol{\eta}_v(t) \tag{5a}$$

$$\dot{\boldsymbol{\beta}}^{true}(t) = \boldsymbol{\eta}_u(t) \tag{5b}$$

Herein, $\boldsymbol{\omega}$ represents the angular rate, $\boldsymbol{\beta}$ the gyroscope bias, $\boldsymbol{\eta}_v$ and $\boldsymbol{\eta}_u$ statistically independent, zero-mean Gaussian white-noise processes.
Fundamental to the Kalman Filter is the observation model $\mathbf{h}(\mathbf{x})$, which serves to establish the relationship between the measurement vector $\mathbf{y}$ and the state vector $\mathbf{x}$. In the context of two unit vector observations, specifically the magnetic field and solar vector, the observation model assumes the following form:

$$\mathbf{y} = \begin{bmatrix} A(\mathbf{q}_{true})\mathbf{r}_1 \\ A(\mathbf{q}_{true})\mathbf{r}_2 \end{bmatrix} + \begin{bmatrix} \boldsymbol{\nu}_1 \\ \boldsymbol{\nu}_2 \end{bmatrix} = \mathbf{h}(\mathbf{x}) + \boldsymbol{\nu} \tag{6}$$

Here, $A(\mathbf{q})$ denotes the rotation matrix corresponding to the quaternion $\mathbf{q}$, while $\mathbf{r}_i$ signifies the reference vectors derived from the applicable mathematical models. The Gaussian zero-mean white noise distribution for each individual vector measurement is represented by the term $\boldsymbol{\nu}_i$. These parameters for the sun and magnetic field vectors define the measurement covariance matrix R, which weights the impact of the measurements on the state estimation.

$$R = \begin{bmatrix} R_1 & 0_{3\times3} \\ 0_{3\times3} & R_2 \end{bmatrix} \tag{7}$$

In this matrix, the assumption is made that the unit vector errors exhibit isotropy, simplifying their representation to $R_i = \sigma_i^2 I_3$.
The particular scenario, in which the payload camera is used as a star tracker, can also be integrated into the observation model of the Kalman filter. The attitude information derived from this source is already presented in the quaternion format and is represented as q_{ST}. The observation model and the measurement covariance matrix R take the following form.

$$\mathbf{y} = 2\frac{(\mathbf{q}^{ST} \otimes \mathbf{q}^{-1})_{1:3}}{(\mathbf{q}^{ST} \otimes \mathbf{q}^{-1})_4} \tag{8a}$$

$$R = \begin{bmatrix} R_1 & 0_{3\times3} & 0_{3\times3} \\ 0_{3\times3} & R_2 & 0_{3\times3} \\ 0_{3\times3} & 0_{3\times3} & R_{ST} \end{bmatrix} \tag{8b}$$

R_{ST} is usually provided by the star tracker itself. The linearized forms of these matrices are presented in detail in [10]. The linearized dynamic equation of the state vector is

$$\Delta\dot{\mathbf{x}}(t) = F(t)\Delta\mathbf{x}(t) + G(t)\mathbf{w}(t) \tag{9}$$

The state transition matrix $F(t)$, $G(t)$ as well as the spectral density $Q(t)$ of the process noise term $\mathbf{w}(t)$ are

$$F(t) = \begin{bmatrix} -[\hat{\boldsymbol{\omega}}(t)\times] & -I_3 \\ 0_{3\times3} & 0_{3\times3} \end{bmatrix} \tag{10}$$

$$G(t) = \begin{bmatrix} -I_3 & 0_{3\times3} \\ 0_{3\times3} & I_3 \end{bmatrix} \tag{11}$$

$$Q(t) = \begin{bmatrix} \sigma_v^2 I_3 & 0_{3\times3} \\ 0_{3\times3} & \sigma_u^2 I_3 \end{bmatrix} \tag{12}$$

The discrete form of the aforementioned matrices is derived in detail in [10] as well as the remaining mathematical properties of the filter.

3.3.1. Verification

The MEKF is verified through simulation of multiple randomly selected initial state conditions. The results, presented in FIG 6, underscore the filter's capability to attain commendable steady-state performance. Even when confronted with unfavorable initial conditions the steady-state acquisition time is in the range of 200 s. The requirement *REQ-1* of 5° performance error is marked as a dotted line. However, it is noteworthy that a minor subset of the initializations resulted in instances of divergence.

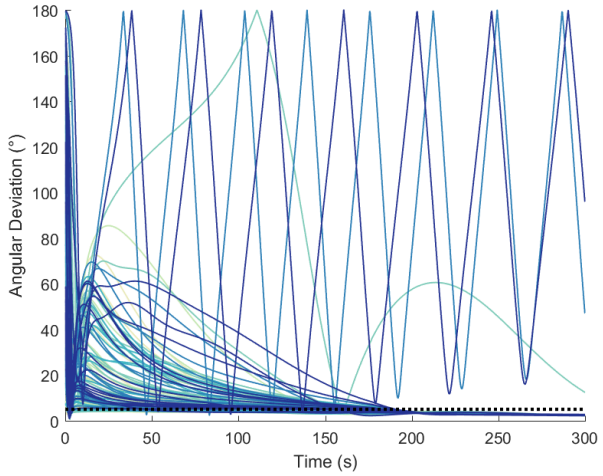

FIG 6. Performance of the MEKF With 100 Random Initial Conditions.

In contrast to the coarse initial filter conditions depicted above, the QUEST algorithm significantly enhanced the convergence, as demonstrated in FIG 7. This enhancement effectively mitigates any concerns of divergence, facilitating the rapid attainment of a stable state that meets the specified performance requirement *REQ-1*.
Note that the accuracy of initialization with the QUEST algorithm varies across the simulation cases. This disparity arises from the inherent connection between the initial satellite orientation and the precision of sun determination — a measurement impacting the overall performance of the QUEST algorithm.
The filter's capability of maintaining the required steady-state performance over the course of several orbits is shown in FIG 8.

4. ATTITUDE CONTROL

Control of SOURCE's attitude is achieved solely by the use of magnetic actuators. A magnetorquer is oriented along each satellite axis. Due to the operating principle of MTQs, torque can only be applied perpendicular to the Earth's magnetic field. Motion parallel to the magnetic field vector can not be altered and needs to be addressed after the orientation of the magnetic field vector has changed sufficiently. This property limits the overall

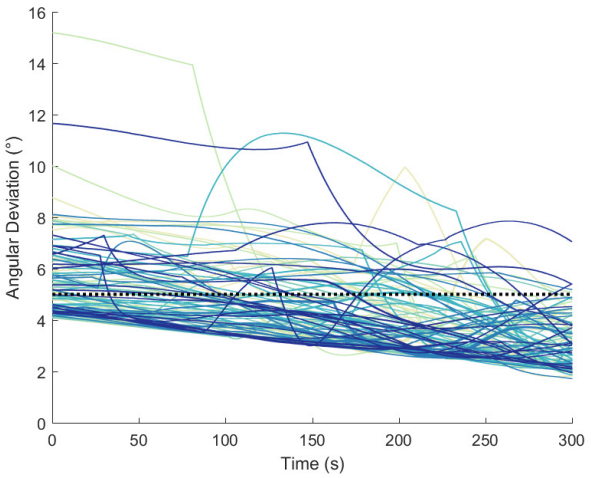

FIG 7. Performance of the MEKF With QUEST For 100 Random Initial Attitudes.

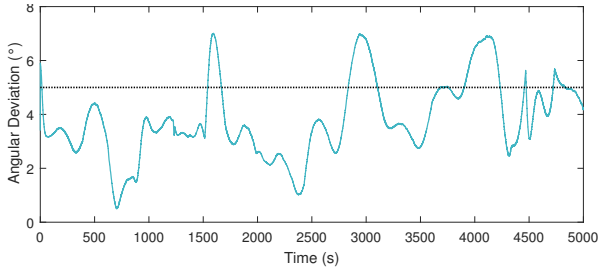

FIG 8. Performance of the MEKF Over Several Orbits.

capability of the system and increases the complexity of control, especially if accurate pointing is required. However, the MTQ-only approach is advantageous in terms of cost, mass, power and volume for CubeSats such as SOURCE. The system operates at 5 Hz and to mitigate interference of the MTQ-produced magnetic field with the MGMs, a preliminary scheduling of 120 ms for actuation and 80 ms for measuring and processing is used for the control cycle of the following simulations.

4.1. Detumble Mode Control

In Detumble Mode, the only sensor used is the MGM. The derivation of the field measurements represent the part of the angular velocity $\omega_{\perp B}$ perpendicular to the magnetic field. The detumble algorithm adopts the approach of monotonously reducing the rotational energy of SOURCE. The selection and stability analysis of the used control law was previously described by F. Tuttas [16]. The *Proportional B-Dot-Law* has been shown to be sufficient for use.

$$\mathbf{m} = -k \cdot \frac{\dot{\mathbf{B}}}{|\mathbf{B}|^2} \tag{13}$$

Here, $\mathbf{m}$ is the magnetic dipole generated by the magnetorquer and $\dot{\mathbf{B}}$ is the derivative of the measured magnetic field vector $\mathbf{B}$. The gain parameter k has been optimized specifically for SOURCE with the use of GAFE.

4.1.1. Verification

The key requirement *REQ-2* for Detumble Mode is to ensure a rotational damping in the time span of 5 h and with separation tip-off rates of up to 90 °s^{-1} on all three axes. In an effort to verify the performance of the used control law, simulations are performed for this initial rotation rate and a typical International Space Station (ISS) orbit.

The in-house developed magnetorquers are tested to produce a minimum of 0.5 A m^2 and they operate in a control cycle with a frequency of 5 Hz [3]. The simulation results over a period of 5 h are shown in FIG 9. As can be seen, the initial rotation of 90 °s^{-1} per axis (≈156 °s^{-1} overall) is completely damped down to below 1 °s^{-1} after about 2 h and 50 min.

If the controller remains active after reaching less than 1 °s^{-1}, the rate of rotation remains stable below this threshold. The target time of less than 5 h is achieved, even with a safety of 1.5. The gain parameter k used in these simulations is $10^{-2.75}$.

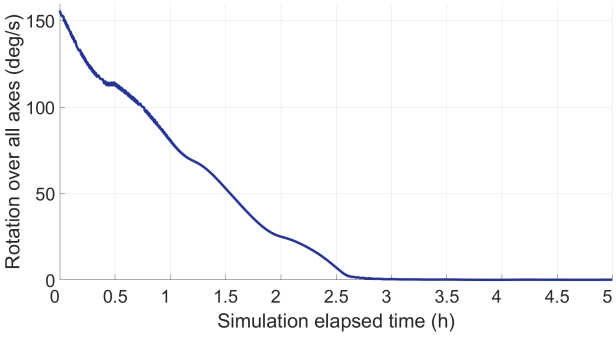

FIG 9. Rotation Rates in Detumble Mode After Deployment Into an ISS Orbit.

A factor that has not been considered in the above simulation is the effect of a residual magnetic dipole moment of the satellite structure itself on the rotational damping in the Detumble Mode. Sources of magnetic dipole moments of the satellite include constant dipoles from the satellite body as well as time-varying dipoles from on-board electronics [17]. Exact measurements of the residual dipole strength for CubeSats are scarce in the literature. However, a good example is Space Dart developed by the U.S. Naval Research Laboratory and Pumpkin Space Systems. Their research team characterised the residual dipole at the Magnetic Test Facility at NASA's Goddard Spaceflight Center. The measured dipole moment of Space Dart was 0.009 A m^2 [18]. Space Dart is a 3U CubeSat with a mass of 5 kg, making it a good comparison with SOURCE due to its similar dimensions and weight, thus allowing a rough estimate of the dipole moment of SOURCE. To evaluate the effect of increasing residual dipole moments on all three body axes on the detumble procedure, multiple GAFE simulations are performed. For this evaluation the simulation setup is identical to the detumble simulation in FIG 9 but with increasing residual magnetic moments. The results for the residual dipole moments on the X$^+$-, Y$^+$- and Z$^+$-axis are shown in FIG 10.

The graphs show that the detumble procedure is capable of damping the rotation below the requirement (dotted line) of 1 °s^{-1} even with residual dipole moments

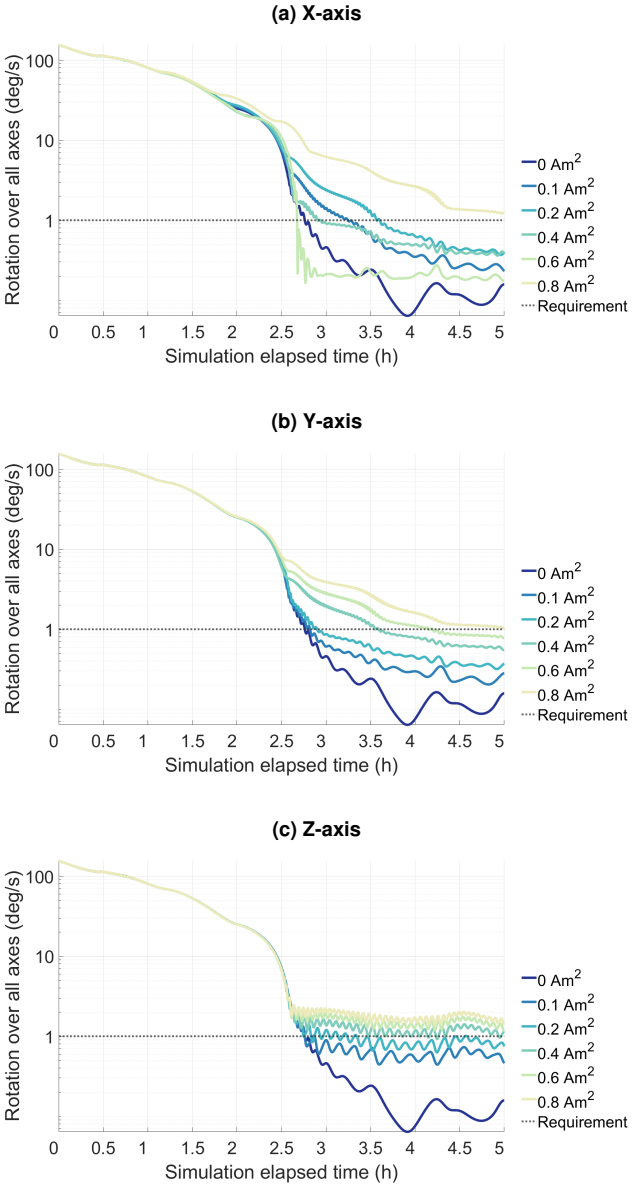

FIG 10. Detumble Test With Disturbances From Residual Magnetic Moments for Each of the Three Axes.

well outside the expected range. The threshold for the residual dipole moment on the X$^+$- or Y$^+$-axis to disrupt the detumble procedure enough to fail the 5 h requirement is approximately 0.8 A m^2. In this scenario, it would have to be stronger than the maximum dipole moment that can be generated by the MTQs at 0.5 A m^2. An exception can be seen when the dipole moment acts on the Z$^+$-axis. In this case, the strength required for the detumble procedure to fail the 5 h requirement is about 0.3 A m^2. These values are between one and two orders of magnitude higher than the measured dipole moment of the Space Dart CubeSat, making it highly unlikely that residual dipole moments would perturb SOURCE to the point of failing to meet the key requirement *REQ-2*. The impact of residual dipole moments on higher operational modes like the Safe Mode requires further investigation.

4.2. Safe Mode Control

In Safe Mode, the primary objective is to stabilize the satellite in case of non-nominal operation and to ensure continuous power generation through sun pointing. It is designed to use a minimum of sensors and only limited processing capacity in order to minimize complexity, power demand and ensure robust operation.
Fundamentally, the control law is laid out as a non-linear PD-type controller. Linearization has been deemed impractical considering that the attitude control system of SOURCE is required to cope with high alignment errors. In Safe Mode, the normal of the solar arrays $\mathbf{s}_{ref}$ (X^+-axis of the body frame, see FIG 1) shall be aligned with the measured sun vector in the body frame $\mathbf{s}$. Additionally, the rotation rate $\boldsymbol{\omega}$ shall be damped. The commanded rotation rate $\boldsymbol{\omega}_{ref}$ is set to zero for use in Safe Mode.
The control law is constructed of an alignment term $\mathbf{M}_{al}$ and a rate damping term $\mathbf{M}_{\omega}$ adding up to the commanded torque $\mathbf{M} = \mathbf{M}_{al} + \mathbf{M}_{\omega}$. The alignment torque is proportional to the angular error between the sun vector and the reference direction of SOURCE. It is defined as

$$\mathbf{M}_{al} = k_{al} \cdot (\mathbf{s}_{ref} \times \mathbf{s}) \cdot \frac{\delta}{\sin(\delta)}. \tag{14}$$

On the other hand the rate damping torque amounts to

$$\mathbf{M}_{\omega} = -\mathbf{K}_{\omega} \cdot (\boldsymbol{\omega} - \boldsymbol{\omega}_{ref}), \tag{15}$$

where $\mathbf{K}_{\omega}$ is constructed as a diagonal 3×3 matrix with identical entries k_{ω} on its principal diagonal. The alignment gain k_{al} is of scalar dimension. Further information on the controller architecture and stability analysis is presented in previous work [3, 16].

4.2.1. Verification

The Safe Mode performance requirement *REQ-3* demands for the normal of the solar panel face to not deviate more than 20° from the sun vector during 68% of the sun phase of the orbit. Furthermore, the rotation rate shall be kept below 1 °s^{-1} after *REQ-4*.
It is necessary to find values for the two gain parameters k_{ω} and k_{al} that satisfy the requirements and optimize the performance. The gain optimization is done using 6-DoF simulations in GAFE. The manual parameter search involves varying both gains on a grid and evaluating the performance after three key parameters. Regions of interest are further analysed by adding additional simulations, refining the grid. To determine the performance of a gain pair, the following criteria are used:

- Time average pointing error (REQ-3)
- Time average rotation rate (REQ-4)
- The proportion of time both the requirements are met.

The last criterion correlates directly to overall performance of the gain pair and is also evaluated in two ways: The total amount of time spent within the safe attitude and the amount of time spent in a safe attitude after the first 5 000 s of the simulation.
The latter is used because it is not clearly defined in the requirement how long the satellite is allowed to take to reach a safe attitude. An acquisition time of 5 000 s corresponds to approximately one full motion through the orbit and is well within the capabilities of the battery to ensure the supply of power during periods of non-optimal power generation.
For this analysis a duration of 10 000 s was used which corresponds to approximately two orbits. The results using a 16x16 grid of gains are shown in FIGs 11 and 12.
The best performing gains are found in the top right corner of the dark region in FIG 12. Another 16x16 grid is placed in the area of $k_{al} = [0.1, 0.32]$ and $k_{\omega} = [1.6 \times 10^{-3}, 4 \times 10^{-2}]$. The results are shown in FIG 13. A further refinement of the gain grid can be seen in FIG 14.
The best performing gains are selected as $k_{al} = -1.5867$ and $k_{\omega} = 0.2267$ and lie within the bright spot in FIG 14. These parameters initially meet the Safe Mode requirement when looking at the time after 5 000 s, since the satellite spends 92% within a safe attitude during the second orbit.

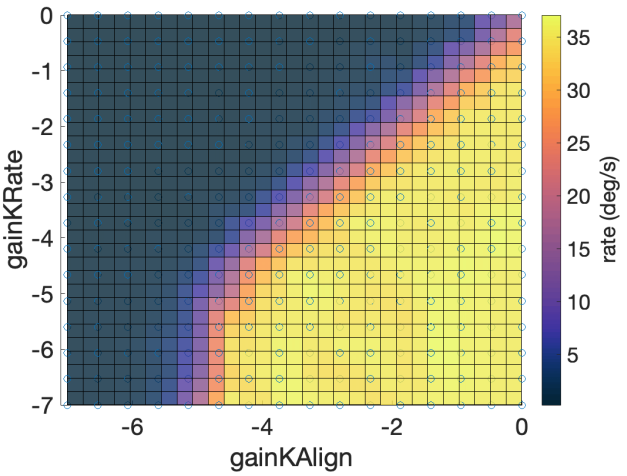

FIG 11. Average Rotation Rate, Coarse Grid (Lower Is Better).

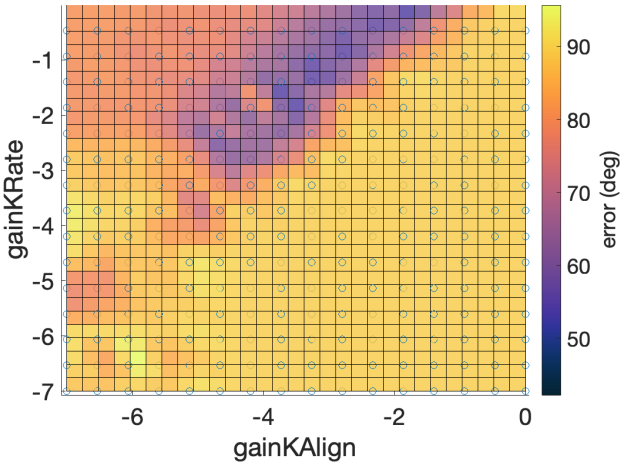

FIG 12. Average Deviation Angle From Sun Vector, Coarse Grid (Lower Is Better).

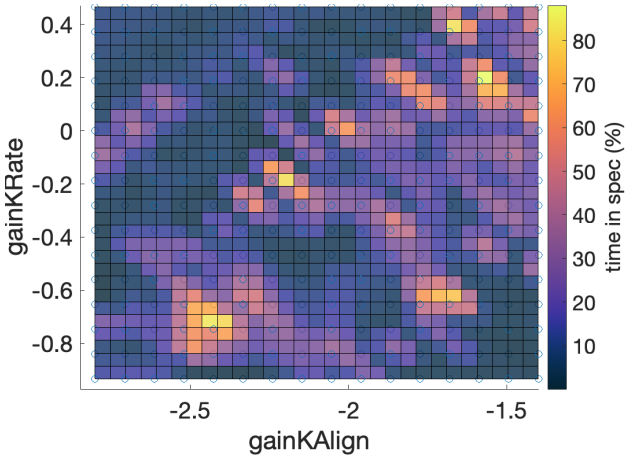

FIG 13. Percentage of Time Within Safe Attitude After First Orbit, Fine Grid (Higher Is Better).

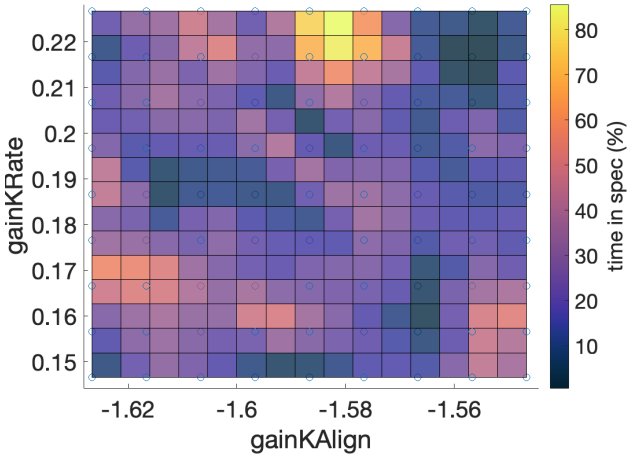

FIG 14. Percentage of Time Within Safe Attitude After First Orbit, Very Fine Grid (Higher Is Better).

Using these best performing gains, the satellite is simulated for 15 000 s, in order to determine whether the controller still performs well for longer duration. In FIG 15 the time series data of the deviation angle and the rotational rate for the three best gain candidates are shown. For this prolonged simulation, the time spent in a safe attitude is 80% for the best gain pair, which satisfies the requirement *REQ-3*. Angular rates are kept below 1 °s^{-1} satisfying *REQ-4*.
To further evaluate the adequacy of these gains, additional simulations need to be performed with a varying set of initial conditions. Thorough Monte-Carlo simulations are planned in order to ensure satisfactory performance and verify a robust controller design.

5. VERIFICATION AND SIMULATION SETUP

As GAFE operates in MATLAB, the algorithms need to be converted to C++ once their performance is confirmed. This conversion is essential for their integration into the flight software. The verification of the flight software is carried out via a separate C++ simulator.
In an effort to test the function of the algorithms in the real world, the code will later be deployed on the OBC and tested in its interaction with the hardware on the

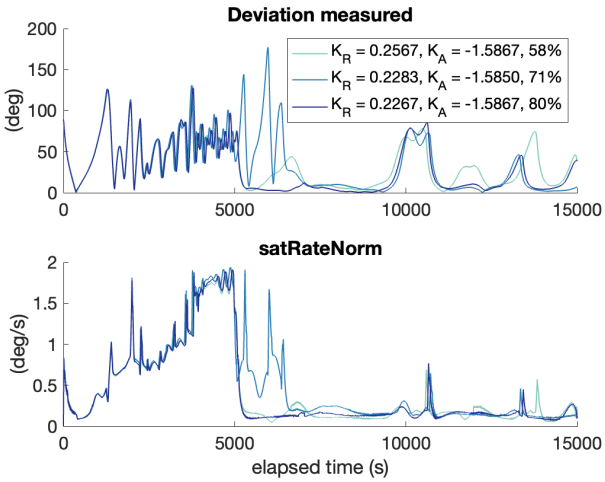

FIG 15. Safe Mode Performance Error Over Three Orbits and the Three Best Gain Pairs.

FlatSat. However, since access to the simulator is limited, an efficient way to test and debug the transpiled software without access to the simulator is executed.
The chosen approach of testing the transpiled ADCS software involves utilizing the MATLAB Mex API, which facilitates the integration of C++ code into MATLAB applications. This permits the incorporation of transpiled modules into the GAFE simulation environment for preliminary verification, before their ultimate integration into the flight software used in the C++ simulator.
Initially, the interface of each individual module with the flight software is established. Each ADCS functionality is isolated within GAFE, allowing for step-by-step verification of the transpiled software. The isolated modules are then transpiled into C++ with respect to the RTOS development requirements. For testing purposes, the existing MATLAB algorithms are replaced with equivalent functions written in C++.
An overview of the integration is given in FIG 16. The validation of the concept is carried out through simulations.

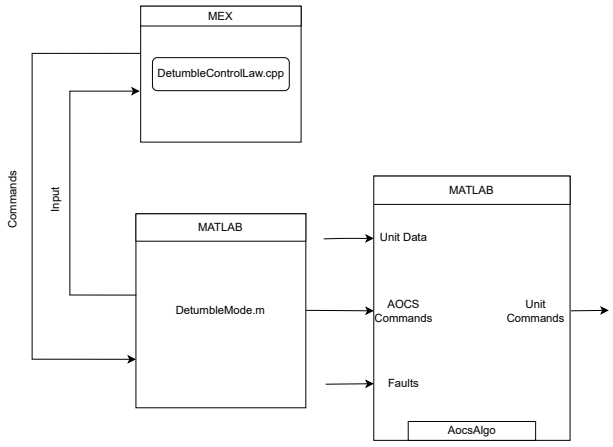

FIG 16. Overview of the C++ Detumble Module Integration Into MATLAB Using MEX.

A comparison of results from the MATLAB and C++ implementations of the detumble control law demonstrated consistent behaviour. This shows that the integration of the C++ code into GAFE is a suitable method for preliminary testing of the transpiled ADCS algorithms by direct comparison with the already verified MATLAB counterpart.

6. RESULTS

The key requirements of SOURCE's ADCS have been shown to be met using the presented laws for attitude determination and control.
Specifically, the results of testing the sun vector algorithm within GAFE have proven that the error is less than 5° when using the pyramid assembly, thus meeting the requirements. The MEKF in combination with the QUEST initialization algorithm was tested to meet the attitude determination requirement. A series of simulations with random initial states show reliable convergence and a stable determination error of less than 5° in the sun phase after an initial acquisition phase. It remains to be seen whether the results can be replicated after transpiling the algorithm into C++.
Regarding control, the detumbling after deployment was shown to be effective and within specifications even with residual dipole moments of the satellite structure well above expected values. The approach to finding, testing and verifying the performance of gains for the Safe Mode control law was presented and observed to yield good results that satisfy the requirements. Further testing needs to be performed, to verify the performance of selected gains. Also other initial flight conditions need to be tested, to evaluate the robustness of the optimized design against higher disturbances and state estimation errors. Further work is required to test the capabilities of the used control law to be used for inertial target pointing.
The early testing of the individual to C++ transpiled ADCS software units within the time domain simulation of GAFE was proven to be effective and useful. The detumble controller was shown to behave identical to the in MATLAB implemented version and thus, verification for the detumble controller is considered successful.
The approach of using GAFE for development and verification of the ADCS algorithms has proven to work well with a student-led CubeSat team. Although initial training and familiarization with the tool may impose a hurdle for incoming students in a project with high personnel fluctuations, distribution of workload into small encapsulated problems turned out to work well.

7. OUTLOOK

The next step towards testing of the ADCS software on the C++ simulator and later in combination with hardware is the transpilation and verification of the system as a whole. Usage of the transpiled control algorithm together with GAFE is tested for the preliminary verification of the C++ conversion before the integration of the ADCS code into the flight software and subsequent testing on the simulator. A FlatSat of SOURCE is currently being built and future effort needs to be undertaken to test the developed software with the real hardware.
Simultaneously, further work has to evolve around a topic that was not discussed in this work: failure detection, isolation and recovery. The ADCS system of SOURCE is desired to be failure-robust to single sensor failures. Thus, strategies for failure detection and handling need to be tested and employed. First tests of this logic can already be performed using GAFE.
Going hand in hand with FDIR are the flight mode transition, that may be triggered by changes of the dynamics of SOURCE due to disturbances and failures. Thorough simulations on various mission scenarios and failure modes need to be carried out in order to verify the overall system performance and robustness.
Lastly, higher modes can be employed in order to increase the capabilities of the ADCS in supporting science. In addition to an already conceptualized Pointing Mode, a Re-entry Mode is envisioned, that not only ensures high quality attitude determination but, also enables altering of the flight condition by either stabilizing or destabilizing SOURCE's attitude motion.
The performance of the ADCS is of upmost importance to the functionality and achievement of the scientific objectives of SOURCE in all mission phases and will therefore continue to be developed with special care to enable a successful mission.

ACKNOWLEDGEMENTS

The authors wish to extend their heartfelt gratitude to all contributing to this unique project - specifically to mention the University of Stuttgart's Institute of Space Systems for their unwavering support, the KSat e.V. and all students for their high level of motivation and engagement - which makes this exceptional hands-on experience of building a satellite possible. Additionally, the team is sincerely thankful to the ESA - Fly Your Satellite! team for their invaluable advice and guidance, which greatly contribute to the success of this project. SOURCE is also supported on behalf of the German Space Agency at the DLR, with funding from the Federal Ministry for Economic Affairs and Climate Action under the funding code 50RU2226, which is highly appreciated by the SOURCE team.

Contact address:

paul.haufe@ksat-stuttgart.de

References

[1] E. Messerschmid and S. Fasoulas. *Raumfahrtsysteme*. Springer, January 2009. ISBN: 978-3-662-49637-4. DOI: 10.1007/978-3-540-77700-7.

[2] E. Kulu. Nanosats Database. www.nanosats.eu. Accessed: 2023-09-11.

[3] N. Maraqten, P. J. Haufe, and M. Zietz et al. Low-Cost Attitude Determination and Control System

of the Student-Built 3U+ CubeSat SOURCE. *International Astronautical Congress*, (IAC-22,E2,3-GTS.4,10,x70167), September 2022.

[4] A. Stier, R. Schweigert, D. Galla, M. Lengowski, and S. Klinkner. Combination of interdisciplinary training in space technology with project-related work through the cubesat source. In *3rd Symposium on Space Educational Activities, Leicester, United Kingdom*, September 2019. DOI: 10.29311/2020.46.

[5] D. Galla, H. Fischer, and P. J. Haufe. In-situ measurements in early phase re-entry of the source cubesat for numerical simulation validation. In *2nd International Conference on Flight Vehicles, Aerothermodynamics and Re-entry Missions & Engineering (FAR)*, Heilbronn, Germany, 2022.

[6] J. C. Springmann, A. J. Sloboda, A. T. Klesh, M. W. Bennett, and J. W. Cutler. The attitude determination system of the RAX satellite. *Acta Astronautica*, 75:120–135, 2012. ISSN: 0094-5765. DOI: 10.1016/j.actaastro.2012.02.001.

[7] N. Maraqten, P. J. Haufe, and C. Vogt et al. A Guide to Self-Built Low-Cost Magnetorquers as will be used in the 3U+ CubeSat SOURCE. *European Cubesat Symposium*, November 2021.

[8] P. J. Haufe. *Aerodynamic Simulation of the SOURCE CubeSat in the Early Re-entry Phase*. Bachelor's thesis, Institute of Space Systems, University of Stuttgart, September 2021.

[9] M. Hirth, H. Su, D. Reggio, and P. Bergner. GAFE User's Manual, Issue 2.1. *European Space Agency*, (GAFE-UM-D7.5b8), August 2018.

[10] F. L. Markley and J. L Crassidis. Fundamentals of Spacecraft Attitude Determination and Control. 2014. DOI: 10.1007/978-1-4939-0802-8.

[11] C. Luckas. *Design and verification of an attitude determination for the student CubeSat SOURCE*. Bachelor's thesis, Institute of Space Systems, University of Stuttgart, 2020.

[12] D. Lang, D. W. Hogg, K. Mierle, M. Blanton, and S. Roweis. Astrometry.net: Blind astrometric calibration of arbitrary astronomical images. *The Astronomical Journal*, 139(5):1782–1800, Mar. 2010. DOI: 10.1088/0004-6256/139/5/1782.

[13] K. Schindler, D. Lang, L. Moore, M. Hümmer, J. Wolf, and A. Krabbe. Computer-aided star pattern recognition with astrometry.net: in-flight support of telescope operations on SOFIA. In Gianluca Chiozzi and Juan C. Guzman, editors, *SPIE Proceedings*. SPIE, Aug. 2016. DOI: 10.1117/12.2231531.

[14] L. Chang and F. Qin. Dynamic analytical initialization method for spacecraft attitude estimators. *CoRR*, June 2017. DOI: 10.48550/arXiv.1706.06814.

[15] N. Pentke, J. Schaefer, T. K. Schwarz, M. T. Koller, S. Gaisser, and S. Klinkner. Comparison of the Low-Cost Sun Sensors of the SOURCE and EIVE CubeSats. In *Small Satellite Conference*, August 2022.

[16] F. Tuttas. *Auslegung des Lageregelungssystems für den Nanosatelliten Student-Operated University Research Cubesat for Education (SOURCE)*. Bachelor's thesis, Institute of Space Systems, University of Stuttgart, December 2018. DOI: 10.13140/RG.2.2.24504.01280.

[17] T. Suehiro. Satellite design methodology to suppress time-varying residual magnet effects on attitude for nano-satellites. *IFAC Proceedings Volumes*, 43(15):241–246, 2010. ISSN: 1474-6670. 18th IFAC Symposium on Automatic Control in Aerospace. DOI: 10.3182/20100906-5-JP-2022.00042.

[18] J. B. Armstrong, C. Casey, G. Creamer, and G. Dutchover. Pointing control for low altitude triple cubesat space darts. In *23rd Annual AIAA/USU Conference on Small Satellites*, 2009.